PATHOGENS AND GLOBAL HEALTH
2022, VOL. 116, NO. 2, 107–118
https://doi.org/10.1080/20477724.2021.1967628



# Effect of HIV aspartyl protease inhibitors on experimental infection with a cystogenic Me49 strain of *Toxoplasma gondii*

Iman Fathy Abou-El-Naga[a], Maha Mohamed Gomaa[a] and Samar Nabil ElAchy[b]

[a]Department Of Medical Parasitology, Faculty Of Medicine, Alexandria University, Alexandria, Egypt; [b]Department Of Pathology, Faculty Of Medicine, Alexandria University, Alexandria, Egypt

**ABSTRACT**

Toxoplasmosis is a zoonotic disease of major significant perspectives in public health and veterinary medicine. So far, the available drugs control only the active infection, once the parasite encysts in the tissues, they lose their efficacy. Cytokines; IFN-γ and IL-10, play a critical role in the modulation of toxoplasmic encephalitis and neuro-inflammation in chronic toxoplasmosis. Antiretroviral protease inhibitors applied in the treatment of acquired immunodeficiency syndrome, revealed activity against multiple parasites. Aluvia (lopinavir/ritonavir) (L/R); an aspartyl protease inhibitor, had efficiently treated *T. gondii* RH strain infection. We investigated the potential activity of L/R against experimental *T. gondii* infection with a cystogenic Me49 strain in mice, considering the role of IFN-γ and IL-10 in the neuropathology versus pyrimethamine-sulfadiazine combination therapy. Three aluvia regimens were applied; starting on the day of infection (acute phase), 2-week PI (early chronic phase) and eight weeks PI (late chronic phase). L/R reduced the brain-tissue cyst burden significantly in all treatment regimens. It impaired the parasite infectivity markedly in the late chronic phase. Ultrastructural changes were detected in *Toxoplasma* cyst membrane and wall, bradyzoite membrane and nuclear envelope. The signs of bradyzoite paraptosis and cytoplasmic lipid droplets were observed. L/R had significantly reduced the brain-homogenate levels of IFN-γ and IL-10 in its three regimens however, they could not reach the normal level in chronic phases. Cerebral hypercellularity, perivascular inflammatory response, lymphoplasmacytic infiltrates and glial cellular reaction were ameliorated by L/R treatment. Herein, L/R was proved to possess promising preventive and therapeutic perspectives in chronic cerebral toxoplasmosis.

**KEYWORDS**

Lopinavir/ritonavir; *Toxoplasma gondii* me49 strain; aspartyl protease inhibitor; cerebral toxoplasmosis; ultrastructural bradyzoite changes; IFN-γ and Il-10 cytokines

## 1. Introduction

Toxoplasmosis is a zoonotic disease affecting more than a billion people. It has a major significance from the perspectives of public health and veterinary medicine. The disease is caused by an obligate intracellular apicomplexan protozoan; *Toxoplasma gondii* (*T. gondii*) [1]. It has high morbidity and mortality impacts, especially in congenitally infected and immunocompromised individuals [2]. Infection of an immunocompetent host is usually asymptomatic, while in immuno-compromised patients; it can develop severe systemic, ocular and neurological disorders. In congenital infections, it is a leading cause of still-birth and congenital defects [3]. Currently, there is no vaccine available to prevent human toxoplasmosis [4].

Human *T. gondii* infection generally occurs *via* ingestion of oocyst-contaminated food or undercooked meat products containing tissue cysts. After ingestion, sporozoites or bradyzoites invade the intestinal cells, where they are converted to tachyzoites and disseminate to remote organs through the hemolymphatic system [5]. Chronic infection develops by conversion of actively replicating tachyzoites into slowly multiplying bradyzoites, which produce intracellular tissue cysts. The progression of *T. gondii* encystation results from both intrinsic reprogramming within the parasite and the immune response of the host, which eventually help to maintain a chronic infection. The brain is the most common chronically affected organ [6]. Chronic non-lethal infection elicited by avirulent *T. gondii* Me49 strain is characterized by modest elevations in T helper 1(Th1) cytokines, which control the infection with minimal damage to the host. More specifically, IFN-γ plays a critical role in the prevention of toxoplasmic encephalitis (TE) during the late stage of infection by inhibiting the proliferation of tachyzoites released from the cysts. Additionally, Th2 cytokine (IL-10) is important to reduce the excessive inflammatory reaction of the brain in chronic toxoplasmosis [7,8].

Antifolate agents; sulfadiazine and pyrimethamine are two primary drugs for the treatment of human toxoplasmosis [9]. Atovaquone has also been used with some success, although its efficacy appeared to be less than pyrimethamine combinations [10]. Alternative therapeutic agents; azithromycin, clarithromycin, trimethoprim/sulfamethoxazole and artemisinin are of variable efficacy [11,12]. So far, there is

**CONTACT** Maha Mohamed Gomaa dr.maha_kh@yahoo.com Department Of Medical Parasitology, Faculty Of Medicine, Alexandria University, Alexandria, Egypt

no available drug capable of eliminating the parasite completely. Some drugs can only limit the multiplication of the parasite during the active stage of replication. However, once the parasite encysts within the tissues, the drugs lose their effectiveness [13]. Furthermore, these therapies can be associated with prominent side effects such as bone marrow depression, hypersensitivity and skin rashes [14]. These shortfalls of the current treatment options necessitate the development of nontoxic, well-tolerated, potent alternatives against the parasite cysts. One of the novel approaches for parasitic treatment is the strategy of repurposing drugs that possess well-characterized pharmacokinetic and safety profiles [15].

The antiretroviral protease inhibitors (APIs) were approved by the US Food and Drug Administration (FDA) for treatment of acquired immunodeficiency syndrome (AIDS) in 2000. They act by competing for the active sites of the protease enzymes [16]. They have markedly reduced the incidence of different opportunistic parasitic diseases, including TE [2]. Previous studies have revealed the antiparasitic activity of APIs against *Plasmodium falciparum, Leishmania spp., Trypanosoma cruzi* [17–19]. Moreover, *in vitro* inhibition of *T. gondii* RH strain had been observed by multiple protease inhibitors such as atazanavir, fosamprenavir, indinavir, nelfinavir, ritonavir and saquinavir [20]. Aluvia; an aspartyl protease (ASP) inhibitor has been successfully tried in the treatment of acute experimental toxoplasmosis [21]. Although this antiparasitic property has been partially attributed to the restoration of cell-mediated immunity, there are evidences that APIs have direct suppressive effects on the proteases of some parasites [16]. Aluvia is one of APIs, composed of lopinavir and ritonavir (L/R), which are used in developing countries for the treatment of AIDS. The main side effects are gastrointestinal disturbances and changes in body fat (fat atrophy and/or deposition) [22].

Bioinformatics identified seven aspartyl protease genes in *T. gondii* and suggested that aspartyl proteases might be a novel drug target for toxoplasmosis treatment [23]. *Toxoplasma* aspartyl protease 5 (ASP5) has fundamental roles at the host-parasite interface. It is essential for maturation of dense granule proteins and formation of the nano-tubular network involved in the parasite lytic cycle [24,25].

In view of the promising in vitro and in vivo antiparasitic activity of ritonavir as one of APIs against the virulent *Toxoplasma* RH strain, the current study was designed to investigate the potential efficacy of L/R 'Aluvia' on experimental *T. gondii* infection with a cystogenic Me49 strain in mice models with an attempt to reveal the role of cytokines (IFN-γ and IL-10) in the neuropathology of the disease.

## 2. Material and methods

### 2.1. Parasite

The cystogenic Me49 strain of *T. gondii* was maintained in the Medical Parasitology Department, Faculty of Medicine, Alexandria University; by serial passage in Swiss albino mice every 2 months. For animal infection, mice were orally inoculated by gavage with brain homogenate suspension containing *T. gondii* cysts (10 cysts/mouse). Eight weeks post infection (PI), mice were anaesthetized with an over-dose of thiopental sodium and sacrificed, brains were homogenized in a glass homogenizer (Wheaton USA) with normal saline. Brain suspensions from chronically infected mice were used for subsequent experimental animal-infection [26].

### 2.2. Drugs

Aluvia tablets (100 mg lopinavir and 25 mg ritonavir) were dissolved in dimethyl-sulfoxide (DMSO) at a final concentration of 10 mg/ml. It was administered orally at a dose of 40 mg/kg/day for two weeks according to a preformed pilot study.

A combination of pyrimethamine (200 mg/kg/day) and sulfadiazine (640 mg/kg/day) was used as a reference therapy. They were individually dissolved in distilled water and administered orally, 8 weeks PI for 2 weeks [27].

### 2.3. Experimental animals

110 male laboratory-bred Swiss albino mice, 4–6 weeks old, weighing 20–25 g were used in the present study. They were maintained in the animal house in a suitable rearing environment, they were housed in metallic, well-ventilated, clean cages. Food pellets and water were continuously supplied and bedding was changed daily. All experimental procedures were conducted in accordance with the Egyptian National Animal Welfare Standards and approved by the Ethics Committee of Alexandria Faculty of Medicine (Approval number: 0304056).

### 2.4. Animal grouping and treatment schedule

Twenty mice were used as a control Group I, which was equally divided into two subgroups (Figure 1). Subgroup Ia (10 non-infected, non-treated, healthy control mice) and subgroup Ib (10 infected, non-treated, control mice). Experimental infection was performed as previously described. Ninety mice served as an experimental Group II, which was further divided into two subgroups. Subgroup IIa included 30 infected, aluvia-treated mice and subgroup IIb included 10 infected, pyrimethamine-sulfadiazine-treated mice (P-S therapeutic control). According to the onset of

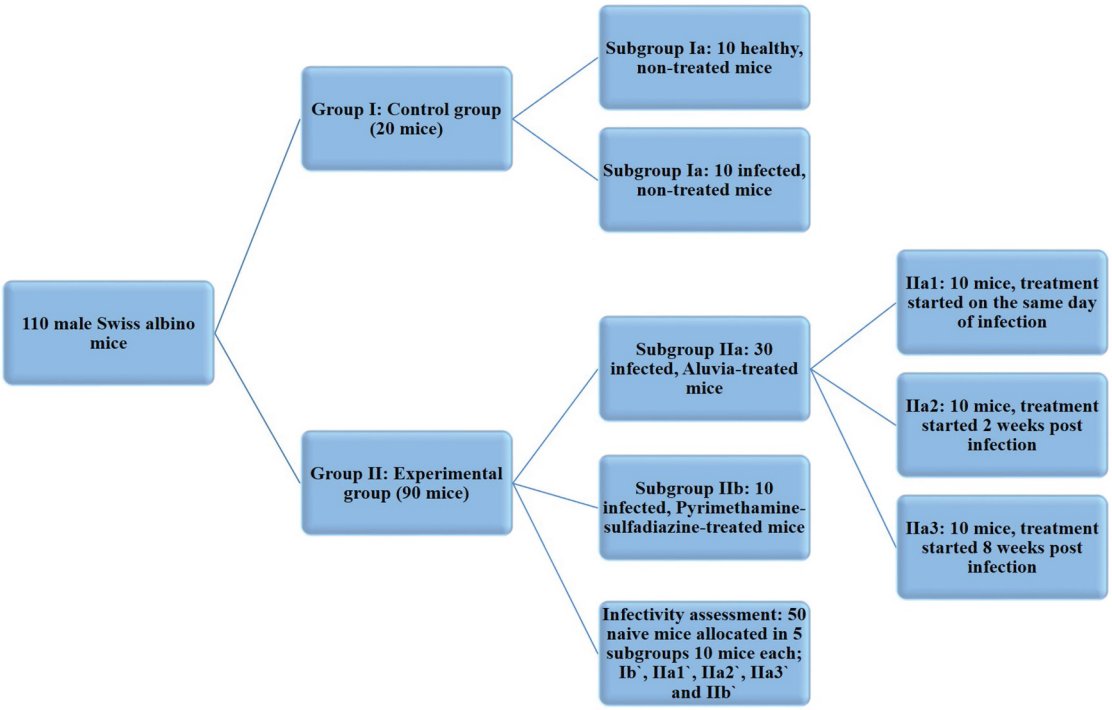


Figure 1. A graphical representation of the different animal studied groups.

treatment, subgroup IIa was equally divided into three subgroups (Figure 1). Subgroup IIa1 included 10 mice and the protective treatment started on the same day of infection. Subgroup IIa2 involved 10 mice and treatment started 2 weeks PI at the early phase of chronic infection. Subgroup IIa3 included 10 mice and treatment started 8 weeks PI at the late phase of chronic infection. The remaining 50 naïve mice were used to assess the infectivity of *Toxoplasma* tissue cysts obtained from the experimentally-infected subgroups, 10 mice for each subgroup. They were named Ib`, IIa1`, IIa2`, IIa3` and IIb`, respectively (Figure 1). Animals of all subgroups were euthanized ten weeks PI.

## 2.5. Assessment of drug efficacy

### 2.5.1. Parasitological study

Observation of food and water intake of all animal subgroups was done on a daily basis and the mortality rate was calculated for each subgroup using the following equation [26]:

$$MR = \frac{\text{Number of deadmice at the sacrifice time}}{\text{Number of mice at the beginning of the experiment}} \times 100$$

To determine the parasite burden, *Toxoplasma* tissue cysts were counted in the brain homogenate of all infected animals and the mean value for each mouse was calculated in 10 high power fields (HPF) with subsequent calculation of the mean value in each subgroup [28]. To assess the parasite infectivity, naïve mice were orally inoculated with brain tissue cysts obtained from the experimentally infected mice, 10 cysts/mouse [29]. Ten weeks later, mice were euthanized and their brain homogenates were separately examined three times under light microscope for *T. gondii* cysts. The infectivity rate (IR) was determined for each subgroup; Ib`, IIa1`, IIa2`, IIa3` and IIb`, by calculating the percentage of mice which were positive for tissue cysts (infected mice) following this equation:

$$IR = \frac{\text{Number of infected mice at the sacrifice time}}{\text{Number of naive mice inoculated with } T.gondii \text{ cysts}} \times 100$$

### 2.5.2. Ultrastructural study

Brain homogenate containing tissue cysts, harvested from subgroup IIa3, was fixed in 2.5% glutaraldehyde and processed for scanning electron microscopy (SEM) and transmission electron microscopy (TEM).

### 2.5.3. Immunological study

Quantitative colorimetric measurement of IFN-γ and IL-10 in brain homogenate of all studied subgroups was performed using mouse IFN-γ ELISA Kit (sigma-aldrich.com) and mouse IL-10 ELISA kit (abcam.com) according to the manufacturer instructions.

### 2.5.4. Histopathological study

Equal parts of the brain tissue (cerebrum) from all the infected animal subgroups were excised, fixed in 10% buffered formalin overnight, processed into paraffin blocks and cut into 5um-thick sections onto glass slides followed by standard Hematoxylin and Eosin (H&E) staining for histopathological examination

under a standard light microscope using x200 and x400 magnifications. Cerebral sections were examined for tissue cysts, perivascular mononuclear infiltration, glial reaction and nodules. The severity of inflammation was scored as four tiers; minimal, mild, moderate and severe in a blinded fashion.

### 2.6. Statistical analysis

Data were analyzed using IBM SPSS software package version 20.0. (Armonk, NY: IBM Corp). The Kolmogorov-Smirnov was used to verify the normality of variables distribution. Comparisons between groups for categorical variables were assessed using Chi-square test (Monte Carlo), ANOVA was used for comparing the four studied groups and followed by Post Hoc test (Tukey) for pairwise comparison. Significance of the obtained results was judged at the 5% level.

## 3. Results

### 3.1. Assessment of the drug efficacy

#### 3.1.1. Parasitological study

There were no abnormal changes in food and water intake in all studied subgroups till the time of authentication (10 weeks PI). Moreover, there was a statistically non-significant difference between the studied subgroups regarding the mortality rate (Table 1). This indicated that the studied drugs as well as the infection with the cystogenic *T. gondii* Me49 strain did not critically affect the animal survival.

The treatment with aluvia had significantly ($P < 0.05$) reduced the parasite burden in terms of the mean *Toxoplasma* cyst count, whenever the onset of its administration, as compared to the infected non-treated subgroup Ib. Moreover, aluvia proved to be statistically superior to P-S combination therapy (IIb) regarding this valuable parameter. The pairwise comparison between every two aluvia-treated subgroups declared statistically significant differences and revealed that subgroup IIa1 was most efficient in reducing the parasite burden (Table 1).

In both animal subgroups IIa1 and IIa2, aluvia could not significantly affect the parasite infectivity ($P > 0.05$) when compared to the infected non-treated control subgroup. Similarly, P-S combination therapy failed to reduce the infectivity of *T. gondii* cysts. Interestingly, treatment with aluvia starting 8-week PI (IIa3) had significantly reduced the parasite infectivity, indicating its direct deteriorating effect on this parasitic stage (Table 1).

#### 3.1.2. Ultrastructural study

SEM showed the non-treated *T. gondii* cysts with spherical shape and smooth regular surface (Figure 2). However, those treated with aluvia 8 weeks PI (IIa3) revealed obvious alterations; irregularities, reduction in size, compressions, deep depressions (Figure 2). Evident protrusions in the cyst wall were also detected (Figure 2)E. The cyst membrane was loose exhibiting a moth-eaten appearance (Figure 2)F. TEM of the non-treated *T. gondii* cyst revealed an intact well circumscribed cyst wall surrounding many bradyzoites with intact cell membranes (Figure 3)-A. Meanwhile, aluvia-treated *T. gondii* cysts (IIa3) demonstrated multiple bradyzoites with marked discontinuity of their plasma membranes (Figure 3-)B. The hallmarks of paraptosis were observed, featuring vacuolation of the bradyzoite; swelling of the mitochondria, dilatation of the endoplasmic reticulum as well as a localized disruption

Table 1. Comparison between the different studied subgroups according to the mortality rate, the cyst count/10 HPF and the infectivity rate.

| | Ia (n = 10) | Ib (n = 10) | IIa1 (n = 10) | IIa2 (n = 10) | IIa3 (n = 10) | IIb (n = 10) | | p |
|---|---|---|---|---|---|---|---|---|
| Mortality rate | 20.0% | 10.0% | 10.0% | 20.0% | 20.0% | 10.0% | | 1.000 |
| Cyst count/ 10 HPF | | | | | | | | |
| Median (Min – Max) | | 10 (8.9–11.8) | 0.9 (0.5–1.4) | 3.1 (2.4–3.8) | 6 (5.2–7.6) | 9.9 (8.8–11) | F = 368.950* | <0.001* |
| Mean ± SD. | | 10.2 ± 0.9 | 0.9 ± 0.3 | 3.1 ± 0.5 | 6.2 ± 0.8 | 9.9 ± 0.7 | | |
| $p_1$ | | | <0.001* | <0.001* | <0.001* | 0.365 | | |
| $p_2$ | | | <0.001* | <0.001* | <0.001* | | | |
| Significance between subgroups | | | $p_3 < 0.001$*,$p_4 < 0.001$*, $p_5 < 0.001$* | | | | | |
| Infectivity rate | | 10 (100%) | 10 (100%) | 8 (80%) | 2 (20%) | 10 (100%) | $x^2 = {}^{2}3.{}^{2}57$* | $^{MC}p<0.001$* |
| $^{FE}p_1$ | | | – | 0.474 | 0.001* | – | | |
| $^{FE}p_2$ | | | – | 0.474 | 0.001* | | | |
| Significance between subgroups | | | $^{FE}p_3 = 0.474$,$^{FE}p_4 = 0.001$*, $p_5 = 0.007$* | | | | | |

$\chi^2$: Chi square test MC: Monte Carlo FE: Fisher Exact
F: F for ANOVA test, pairwise comparison between each two subgroups was done using Post Hoc Test (Tukey)
p: p value for comparing between the different studied subgroups
$p_1$: p value for comparing between Ib and IIa1, IIa2, IIa3, IIb
$p_2$: p value for comparing between IIb and IIa1, IIa2, IIa3
$p_3$: p value for comparing between IIa1 and IIa2
$p_4$: p value for comparing between IIa1 and IIa3
$p_5$: p value for comparing between IIa2 and IIa3
*: Statistically significant at $p \leq 0.05$
Ia: Healthy control, Ib: Infected control, IIa1: Aluvia-treated (day zero), IIa2: Aluvia-treated (second week), IIa3: Aluvia-treated (eighth week), IIb: Therapeutic control

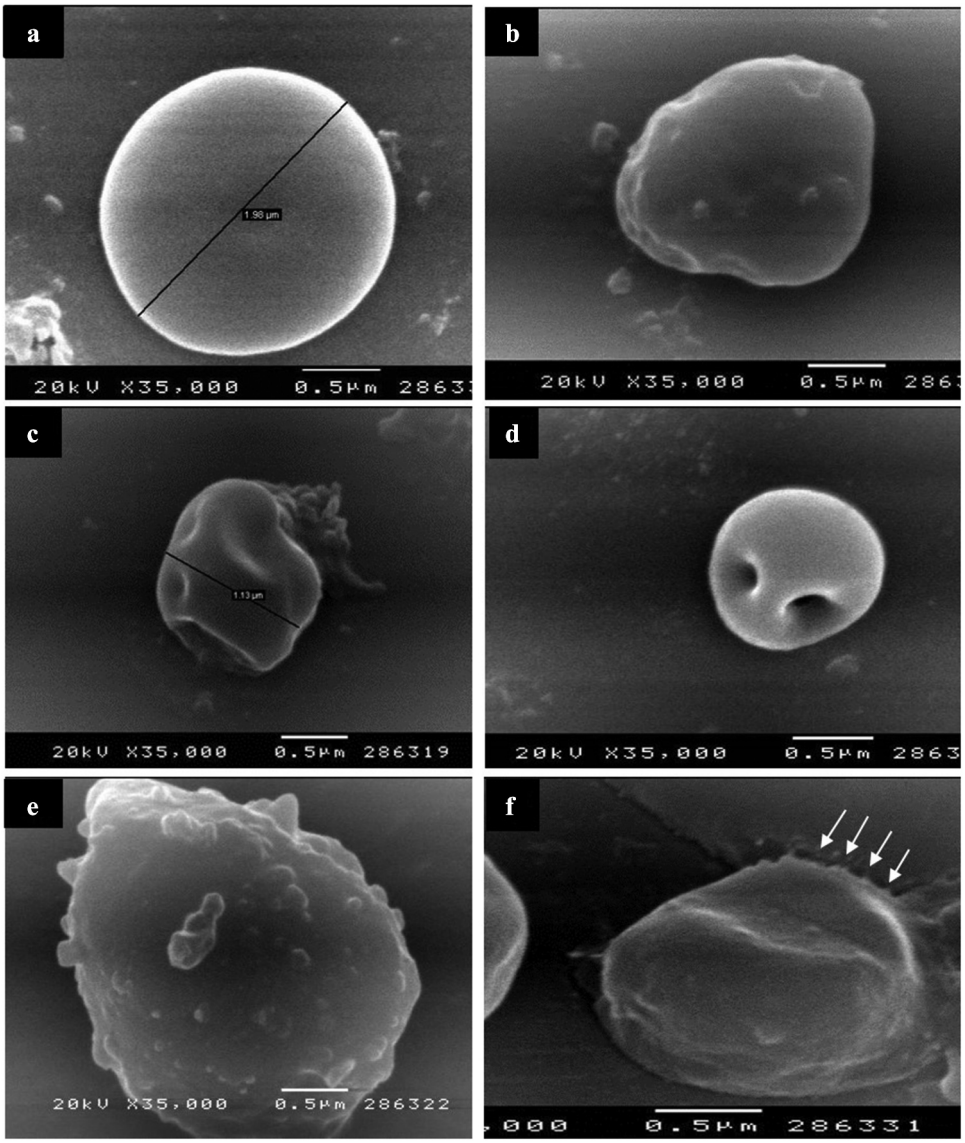


Figure 2. SEM of *T. gondii* cysts in brain homogenate of the avirulent Me49 strain-infected non-treated subgroup (Ib) (A) and the infected aluvia-treated one (IIa3) (B-F). (A) Non-treated *T. gondii* cyst possessing a spherical shape, a regular surface and 1.98 µm diameter. (B) Aluvia-treated *T. gondii* cyst showing irregularities and multiple nearby compressions of the cyst wall. (C and D) *T. gondii* cysts revealing their small size (1.13 µm diameter) with shallow and deep depressions in their surface. (E) *T. gondii* cyst demonstrating multiple cyst wall protrusions. (F) *T. gondii* cyst having a redundant disrupted cyst membrane with a moth-eaten appearance at one side (arrows).

of the nuclear envelope (Figure 3)-C. Lipid droplets of varying sizes and electron densities were also identified (Figure 3)-C and D.

### 3.1.3. Immunological study

Regarding the brain-homogenate level of IFN-γ (Table 2), both the infected non-treated (Ib) and pyrimethamine-sulfadiazine-treated (IIb) subgroups showed almost a one-fold rise, which was statistically significant ($P < 0.001$) as compared to the healthy control subgroup (Ia). However, the level of IFN-γ in subgroup IIb was not significantly affected, when compared to subgroup Ib. Notably, the three aluvia-treated subgroups IIa1, IIa2 and IIa3 recorded statistically significant reductions, c whether ompared to subgroup Ib or subgroup IIb. Notably, the IFN-γ concentration had approximated the normal level in subgroup IIa1, relative to the healthy subgroup Ia ($P = 0.454$). Contrarily, it remained significantly higher than the normal level in both early and late chronic phases of aluvia therapeutic regimens (IIa2 and IIa3) ($P = 0.008$ and $P < 0.00$, respectively). In a pairwise comparison between aluvia-treated subgroups, the IFN-γ level of subgroup IIa3 was significantly higher than the two other subgroups.

As regards IL-10 (Table 2), pyrimethamine-sulfadiazine regimen (subgroup IIb) did not affect its level in the brain homogenate obviously when compared to the infected non-treated controls (Ib) ($P = 0.480$). Both subgroups Ib and II b recorded about a five-fold rise, which was statistically significant ($P < 0.001$) when compared to the healthy controls (Ia). All subgroups treated with aluvia showed significantly reduced levels of IL-10 in

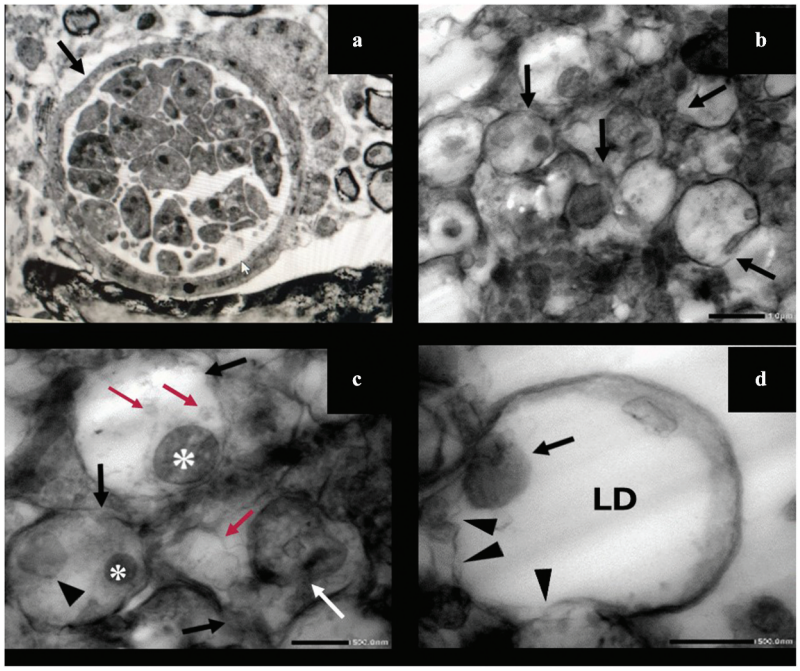


**Figure 3.** TEM of *T. gondii* cysts in brain homogenate of the avirulent Me49 strain-infected non-treated subgroup (Ib) (A) and the infected aluvia-treated one (IIa3) (B-D). (A) *T. gondii* cyst revealing an intact well circumscribed cyst wall (arrow) containing multiple bradyzoites with intact cell membranes (x 3000). (B) Multiple *T. gondii* bradyzoites showing disrupted plasma membranes (arrows) (x 5000). (C) Bradyzoites demonstrating marked discontinuity of their plasma membranes (black arrows), lipid droplets of varying sizes and densities (red arrows), swollen mitochondria (asterisks), dilated endoplasmic reticulum (arrow head) and a localized disruption of the nuclear envelope (white arrow) (x 15,000). (D) A bradyzoite possessing a swollen mitochondrion (arrow) and a large electron-lucent lipid droplet (LD) with evident disintegration of its plasma membrane (arrow heads) (x 20,000).

**Table 2.** Comparison between the different studied subgroups according to the level of IFN-gamma and IL-10 in brain homogenate.

| | Ia (n = 10) | Ib (n = 10) | IIa1 (n = 10) | IIa2 (n = 10) | IIa3 (n = 10) | IIb (n = 10) | F | p |
|---|---|---|---|---|---|---|---|---|
| IFN-gamma (pg/ml) | | | | | | | | |
| Median (Min – Max) | 1.1 (0.8–1.1) | 1.9 (1.7–2.2) | 1.1 (1–1.4) | 1.3 (1–1.5) | 1.7 (1.5–1.9) | 1.9 (1.7–2.1) | 62.602* | <0.001* |
| Mean ± SD. | 1 ± 0.1 | 1.9 ± 0.2 | 1.1 ± 0.2 | 1.3 ± 0.2 | 1.7 ± 0.2 | 1.9 ± 0.2 | | |
| $p_1$ | | <0.001* | 0.454 | 0.008* | <0.001* | <0.001* | | |
| $p_2$ | | | <0.001* | <0.001* | 0.010* | 1.000 | | |
| $p_3$ | | | <0.001* | <0.001* | 0.028* | | | |
| Significance between subgroups | | | $p_4 = 0.480, p_5 < 0.001^*, p_6 < 0.001^*$ | | | | | |
| IL-10 (ng/ml) | | | | | | | | |
| Median (Min – Max) | 1.3 (1–1.5) | 7.9 (7.6–8.3) | 2.7 (2–3) | 4 (3.5–4.3) | 5.9 (5.3–6.3) | 7.7 (6.9–8.5) | 875.150* | <0.001* |
| Mean ± SD. | 1.3 ± 0.2 | 7.9 ± 0.2 | 3 ± 2.6 | 4 ± 0.3 | 5.9 ± 0.4 | 7.7 ± 0.2 | | |
| $p_1$ | | <0.001* | <0.001* | <0.001* | <0.001* | <0.001* | | |
| $p_2$ | | | <0.001* | <0.001* | <0.001* | 0.480 | | |
| $p_3$ | | | <0.001* | <0.001* | <0.001* | | | |
| Significance between subgroups | | | $p_4 < 0.001^*, p_5 < 0.001^*, p_6 < 0.001^*$ | | | | | |

F: F for ANOVA test, a pairwise comparison between each two subgroups was done using Post Hoc Test (Tukey)
p: p value for comparing between the different studied subgroups
$p_1$: p value for comparing between Ia and Ib, IIa1, IIa2, IIa3, IIb
$p_2$: p value for comparing between Ib and IIa1, IIa2, IIa3, IIb
$p_3$: p value for comparing between IIb and IIa1, IIa2, IIa3
$p_4$: p value for comparing between IIa1 and IIa2
$p_5$: p value for comparing between IIa1 and IIa3
$p_6$: p value for comparing between IIa2 and IIa3
*: Statistically significant at $p \leq 0.05$
Ia: Healthy control, Ib: Infected control, IIa1: Aluvia-treated (day zero), IIa2: Aluvia-treated (second week), IIa3: Aluvia-treated (eighth week), IIb: Therapeutic control

comparison to the infected and therapeutic controls (Ib and IIb). However, they did not reach the normal level as they recorded approximately one-fold, two-fold and three-fold rises, respectively. Interestingly, when comparing between the three aluvia-treated subgroups, a statistically significant difference between every two subgroups was observed, verifying the remarkable difference between the three aluvia treatment regimens.

### 3.1.4. Histopathological study

Histopathological examination of H&E stained cerebra obtained from *T. gondii* Me49 strain-infected mice revealed normal cerebral structure without obvious alterations of their architecture and normal neuronal bodies in the gray matter. The infected non-treated controls (Ib) and the infected pyrimethamine-sulfadiazine-treated ones (IIb) demonstrated cerebral hypercellularity caused by the diffuse reactive gliosis and mononuclear inflammatory reaction featuring lymphoplasmacytic infiltrates in a perivascular predisposition (Figure 4-A-C). *T. gondii* bradyzoites were encountered in the white matter inside well-defined cyst walls, a diffuse glial reaction and localized microglial nodules were also detected (Figure 4-D and E). Additionally, foci of vascular proliferation were identified in terms of increased number of small proliferating vessels with proliferated hypertrophied endothelial lining (Figure 4-F). Many reactive astrocytes were clearly observed within the cerebral tissue (Figure 4-G). However, in the infected aluvia-treated subgroup IIa1, *T. gondii* cysts with well-

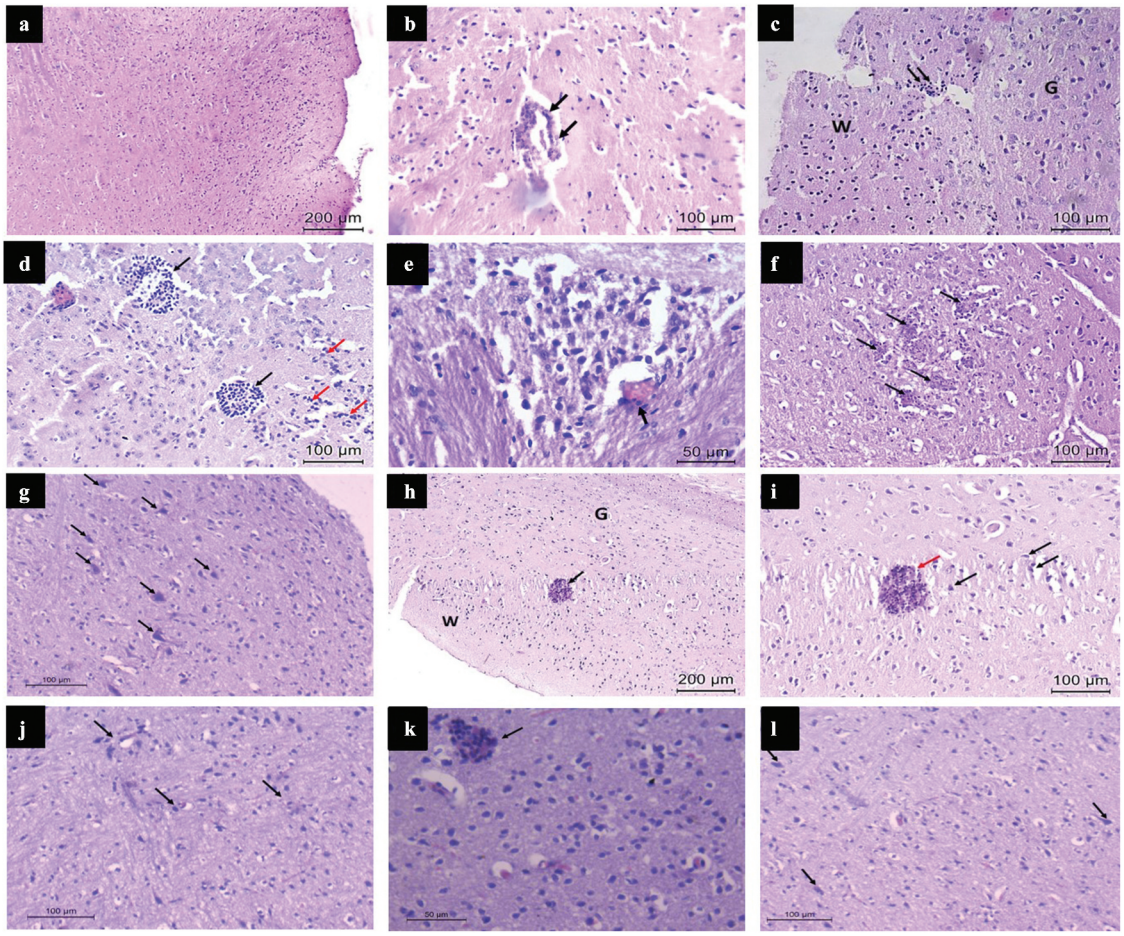


Figure 4. Histopathologic examination of the hematoxylin and eosin-stained cerebra, obtained from *Toxoplasma gondii* Me49 strain-infected mice (Infected non-treated, infected aluvia-treated and infected pyrimethamine-sulfadiazine-treated subgroups; Ib, IIa and IIb, respectively). Subgroups Ib and IIb (A-G), subgroup IIa1 (H and I), subgroup IIa2 (J) and subgroup IIa3 (K and L). (A) A photomicrograph revealing the normal structure of the cerebrum without obvious alterations of its architecture as well as cerebral hypercellularity caused by the diffuse glial reaction and mononuclear inflammatory infiltrates. (B) A photomicrograph showing cerebral perivascular lymphoplasmacytic infiltrates (arrows). (C) A photomicrograph demonstrating reactive gliosis in the cerebral white matter (W) with perivascular mononuclear inflammatory infiltration (arrows) and normal neuronal bodies in the gray matter (G). (D) A photomicrograph showing *T. gondii* bradyzoites (black arrows), encountered in the cerebral white matter, having well-defined cyst walls with nearby reactive glial cells and lymphoplasmacytic infiltrates (red arrows). (E) A high power view revealing a localized microglial nodule, as well as a perivascular lymphocytic infiltrate (arrow). (F) A photomicrograph showing foci of vascular proliferation (arrows) in the form of increased numbers of small proliferating vessels as well as proliferated hypertrophied endothelial lining. (G) A photomicrograph showing reactive astrocytes (arrows) with diffuse mononuclear inflammatory cellular infiltrates. (H) A photomicrograph demonstrating a *T. gondii* tissue cyst (arrow) in the cerebral white matter (W) possessing a well-defined cyst wall, surrounded by a mild glial reaction and minimal lymphoplasmacytic infiltrates, the gray matter (G) shows normal neuronal bodies. (I) A high power view revealing a *T. gondii* tissue cyst (red arrow) with a well-defined cyst wall and surrounded by a mild glial cellular reaction (black arrows). (J) A photomicrograph showing mild mononuclear inflammatory cellular infiltrates predominantly in a perivascular distribution (arrows). (K) A photomicrograph showing moderate mononuclear inflammatory cellular infiltrates in the cerebral cortex with a *Toxoplasma* tissue cyst filled with bradyzoites (arrow). (L) A photomicrograph showing reactive astrocytes (arrows) and moderate mononuclear inflammatory infiltrates.

defined walls were detected, they were only surrounded by a mild glial cellular reaction and minimal lymphoplasmacytic infiltrates (Figure 4)H and I. In subgroup IIa2, a mild mononuclear inflammatory infiltration predominantly in a perivascular distribution was encountered (Figure 4-J). In subgroup IIa3, a moderate mononuclear inflammatory infiltrates in the cerebral cortex, bradyzoites-filled tissue cyst and few reactive astrocytes were observed (Figure 4-K and L). These observations demonstrate a remarkable amelioration of the chronic neuroinflammatory tissue response following the treatment with aluvia.

## 4. Discussion

An ultimate goal in the treatment of chronic toxoplasmosis is to find drugs with dual activity against the active replicative stage and the cystic stage of the parasite. Previously, we demonstrated that L/R was effective against tachyzoites in acute toxoplasmosis [21]. Herein, we revealed its additional effect on the latent parasitic stage in chronic toxoplasmosis.

The low oral dose [10 cysts/mouse) of the avirulent *T. gondii* Me49 strain used for experimental infection in the present study did not critically affect the animal survival in all studied subgroups. This is supported by 26. Mortality rate reached 60–65% by the end of 7$^{th}$ week of infection due to encephalitis upon intraperitoneal inoculation of a higher dose (20 cysts/mouse] of the same parasite strain [29].

In the present study, treatment with aluvia showed an obvious protective effect against chronic toxoplasmosis when started concomitantly with the infection (subgroup IIa1) and sustained for two weeks. During this period, the drug seemed to act on the newly-released bradyzoites and rapidly replicating tachyzoites. The drug proved the therapeutic activity in the early and late chronic phases of the disease. At the early chronic phase (two weeks PI), aluvia was acting on young tissue cysts containing moderately active bradyzoites. Newly formed cysts in the brain were detected 2 weeks PI and reached the maximum count after 4 weeks [30]. Treatment was also effective at the late chronic phase (8 weeks PI), fighting against mature cysts containing slowly dividing bradyzoites [30]. Aluvia recorded a descending statistically significant reduction in the brain cyst burden in the subgroups IIa1, IIa2 and IIa3 compared to the infected control subgroup. Similarly, atovaquone and auranofin showed a higher therapeutic efficacy in the early stage of infection with *T. gondii* cystogenic strain than the late stage [10,15]. Aluvia, like other drugs being investigated against Me49 strain of *T. gondii*, did not achieve the desired goal of complete clearance of parasitic cysts due to the protective effect of their walls [26,31,32].

Mature brain cysts, obtained from subgroups IIa1and IIa2, were able to re-infect naïve mice. The obvious reduction in the cyst count with retained infectivity in such subgroups could be explained by the high potential killing effect of aluvia on the metabolically active, multiplying, early parasitic stages. While, the remaining parasites that circumvent the drug, could reach the brain and develop infective cysts. The diminution of mature cysts' infectivity was clearly achieved by aluvia in the late chronic phase (subgroup IIa3). It seemed to possess a direct deteriorating effect on the dormant parasitic stage in the late chronic phase after cyst-wall formation. This is of substantial importance in the context of reducing the incidence, prevalence and severity of TE following treatment of AIDS patients with L/R. Moreover, in immunocompetent hosts, tissue cysts may occasionally rupture leading to the release of some parasites [33]. The reduction of cyst burden and infectivity elicited by aluvia, could ultimately lower the risk of disease reactivation, attenuate the re-infection power of the latent parasite and so, protect against occurrence of fatal encephalitis.

The deterioration of parasite growth, multiplication and re-infection after treatment with aluvia could be attributed to its inhibitory effect on ASP enzymes, whose coding genes were described in *T. gondii* [23]. *T. gondii* ASP5 is a Golgi-resident protease, essential for proper protein transport and its absence markedly compromises the parasite's ability to modulate host signaling pathways. Knockout of this enzyme affects the parasite growth, decreases its virulence, fitness and impairs its spontaneous egress, which enables parasite to escape the membrane of an infected expiring host cell to infect a new target one [25,34]. Treatment of acute toxoplasmosis with L/R decreased tachyzoite egress from infected cells, preventing repeated cycles of cell invasion and intracellular replication. Moreover, it elicited disruption of the nano-tubular network within the PV enclosing tachyzoites [21]. The dense granule proteins (GRA) are essential for the construction of this network which is important in nutrient acquisition and formation of a membranous parasite-host cell interface [35]. Under the control of *Toxoplasma* ASP5, the parasite secretes proteins into PV to breach the enclosing membranous system [36]. In *Plasmodium* biology, the egress was a protease-dependent function and protease inhibition by lopinavir lead to transmission-blocking effect [37,38]. Similarly, in retrovirus infection, lopinavir competes for binding to the cleavage site within the ASPs leading to the release of noninfectious viral particles with subsequent regression of the disease [39].

After differentiation of tachyzoites into bradyzoites, PVM is retained as a cyst membrane, surrounding a thick cyst wall [40,41]. Herein, at the late chronic phase of infection, the ultrastructural changes in the

cyst size, wall and membrane as well as in bradyzoites' plasma membranes might be also explained by the inhibitory effect of lopinavir on *Toxoplasma* ASPs. These enzymes are crucial for the biological functions of highly expressed *Toxoplasma* GRA proteins. Many of these proteins are substrates of *Toxoplasma* Golgi complex-associated ASP5 [34]. The knockout of such an enzyme-coding gene impaired the cyst wall formation after in vitro tachyzoite-bradyzoite conversion [25]. GRA are crucial for cyst-membrane maturation, accumulation of cyst wall cargo, development of cyst wall and matrix so, their defective production could eventually affect these structures [41–43]. Deletion of *Toxoplasma* cyst GRA4 and/or GRA6 have drastically reduced tissue cyst burdens in murine brains [44]. Both GRA17 and GRA23 functions synergistically to facilitate PVM permeability and nutrient access [45]. Therefore, defective cleavage of such proteins could suppress bradyzoite growth and replication and so, reduce brain cyst size in subgroup IIa3. Furthermore, GRA17 is essential for bradyzoite viability inside the cysts [46].

Beside the assumed inhibitory effect of aluvia on *Toxoplasma* ASPs, it could exert its effect through different pathways. Herein, TEM revealed lipid droplets, varying in size and electron density inside the bradyzoites following treatment with aluvia, suggesting an altered parasite lipid storage and metabolism which may arrest the parasite development. Similar findings were reported in *Leishmania amazonensis* promastigotes and *T. cruzi* trypomastigotes after treatment with lopinavir [19,47]. We observed that aluvia induced paraptotic changes with vacuolization of bradyzoite endoplasmic reticulum and mitochondrial dilatation. Similar changes were reported in *T. gondii* tachyzoites and *T. cruzi* trypomastigotes after treatment with such a drug [19,21]. However, it remains possible that aluvia can reduce the energy of *T. gondii* parasite in ways that contribute to the observed results. *Plasmodium falciparum* was killed by lopinavir through the inhibition of the glucose transporter, thus decreased the parasite glucose-uptake which is the primary source of its energy [48].

In the current study, toxoplasmosis elicited a high level of IFN-γ in the brain homogenate of infected non-treated control mice (Ib). In the brain, microglia are the first line of defense against parasite spread, through IFN-γ secretion, which inhibits tachyzoite growth, proliferation and prevents reactivation of infection at the chronic stage [49]. A fine balance between host immunity and immune evasion of the parasite leads to establishment of the chronic infection [8]. IFN-γ controls the intracellular multiplication of the tachyzoite by effector molecules including indoleamine-2,3-dioxygenase-1 [50] and nitric oxide [51,52]. It also induces expression of endothelial vascular adhesion molecule-1 on cerebral vessels, to recruit T cells during chronic infection [53]. This fact could justify the cerebral hypercellularity, perivascular mononuclear inflammatory reaction and lymphocytic infiltrates, observed in brain-tissue sections in the infected non-treated control mice (Ib). Furthermore, astrocytes played an obvious contributing role in IFN-γ secretion in our work, as proved by their evident reactive appearance in cerebral histopathology of such a subgroup. $CD8^+$ T cells have a powerful protective activity, they can remove *T. gondii* cysts from the brain independently of IFN-γ production. This is through a perforin-mediated cytotoxicity, which leads to destruction of the cysts, followed by activation and accumulation of microglia and macrophages for their elimination [54]. In our study, this phenomenon could give an evidence for the presence of focal microglial nodules in cerebral tissue of subgroup Ib animals. *Toxoplasma* cysts are not static structures; they regularly breakdown and reinvade nearby host cells, eliciting an inflammatory response, forming such glial nodules in chronic infection [55].

A significant increase in the level of IL-10 was detected in the brain homogenate of chronically infected non-treated mice. IL-10 functions in a host-protective manner. It does not directly control the parasite growth but it is crucial for downregulation of IFN-γ-mediated immune responses and prevention of the immune-pathological sequels in *Toxoplasma* infection. The induction of IFN-γ and the regulatory effect of IL-10 are key elements in host resistance to *Toxoplasma* parasite [56]. IL-10 is produced mainly by IFN-γ-secreting T-bet$^+$Foxp3$^-$ Th1 cells so, its production by Th1 cells offers an important negative-feedback loop to prevent the immune-pathologic overstimulation of the Th1 in response to *Toxoplasma* [57].

Impaired activity of several GRA proteins by aluvia might be a leading cause of increased parasite-vulnerability to the killing effect of IFN-γ. GRA12 underpins the resistance to host IFN-γ in chronic toxoplasmosis [42]. GRA15 antagonizes the anti-parasitic effect of IFN-γ, by suppressing indoleamine-2,3-dioxygenase-1 in the brain [58]. The latter possesses an inhibitory effect on *Toxoplasma* growth through starvation for tryptophan [59]. Notably, ASP5 is also required for the export of *T. gondii* inhibitor of STAT1 transcription activity (TgIST) to the host cell nucleus. TgIST possesses a suppressive effect on IFN-γ gene expression by host cells [60].

Herein, the significantly-decreased levels of IFN-γ and IL-10 in the brain homogenate after treatment with aluvia (subgroups IIa1, IIa2 and IIa3) relative to the infected non-treated control subgroup, appeared to be concomitant with the reduction of parasite burden. Notably, in both early and late chronic phases (IIa2 and IIa3), both cytokine levels did not return to the normal level because aluvia falls short of eradicating the infection entirely. The efficient parasite control depends on the induction of $CD8^+$ T cell response,

specific for immunodominant GRA6 which plays an evident role in cytogenesis [61]. Furthermore, presentation of GRA6 by neuronal major histocompatibility complex-1 is pivotal for restricting *T. gondii* in the brain during chronic phase [62]. This is elicited by continuous production of effector $CD8^+$ T cells through a proliferative subset with a phenotype possessing combined features of memory and effector T cells [62,63]. Hence, the remaining parasites which circumvent aluvia, stimulate these cells to maintain a continued production of IFN-γ as well as the regulatory IL-10, keeping their levels higher than the healthy control group. Interestingly, L/R improved the cytokine-storm and reduced the level of IFN-γ and IL-10 in response to COVID-19 [64,65]. Lopinavir had reduced the anti-inflammatory profile of macrophages in *Leishmania* infection by diminishing IL-10 secretion [66].

In conclusion, the current study revealed the preventive and the therapeutic efficacy of aluvia on chronic cerebral toxoplasmosis. The dual activity against tachyzoites and bradyzoites, the reduction in the cyst burden, the impairment of cyst infectivity, the reduced levels of IFN-γ and IL-10 relative to the infected untreated controls, together with the amelioration of neuropathology in the chronic phases, could avoid the risk of life-threatening disease reactivation and could explain the reduced incidence of TE in HIV-infected patients treated with L/R. It is of utmost importance to study the effect of such a drug in immunocompromised animal model.

## Acknowledgments

The authors wish to thank Dr. Ashraf Barakat, Zoonotic Department, National Research Centre, Cairo, Egypt for kind providing of *T. gondii* Me49 strain.

## Disclosure statement

No potential conflict of interest was reported by the author(s).

## Funding

This research did not receive any specific grant from funding agencies in the public, commercial, or not-for-profit sectors.

## ORCID

Maha Mohamed Gomaa http://orcid.org/0000-0002-6526-5814

## References

[1] Dubey JP. Toxoplasmosis of Animals and Humans. Second ed. Boca Raton, Florida: CRC Press Inc; 2010. p. 1–313.
[2] Pereira-Chioccola VL, Vidal JE, Su C. *Toxoplasma gondii* infection and cerebral toxoplasmosis in HIV-infected patients. Future Microbiol. 2009;4:1363–1379.
[3] Elsheikha HM. Congenital toxoplasmosis: priorities for further health promotion action. Public Health. 2008;122:335–353.
[4] Chu KB, Quan FS. Advances in *Toxoplasma gondii* vaccines: current strategies and challenges for vaccine development. Vaccines (Basel). 2021;9:413–428.
[5] Harker KS, Ueno N, Lodoen MB. *Toxoplasma gondii* dissemination: a parasite's journey through the infected host. Parasite Immunol. 2015;37(3):141–149.
[6] Wohlfert EA, Blader IJ, Wilson EH. Brains and brawn: *toxoplasma* infections of the central nervous system and skeletal muscle. Trends Parasitol. 2017;33:519–531.
[7] Cerutti A, Blanchard N, Besteiro S. The bradyzoite: a Key developmental stage for the persistence and pathogenesis of toxoplasmosis. Pathogens (Basel. Switzerland). 2020;9(3):234.
[8] Suzuki Y, Sa Q, Gehman M, et al. Interferon-gamma- and perforin-mediated immune responses for resistance against *Toxoplasma gondii* in the brain. Expert Rev Mol Med. 2011;4:13–31.
[9] Rodriguez JB, Szajnman SH. New antibacterials for the treatment of toxoplasmosis; a patent review. Expert Opinion on Therapeutic Patents. 2012;22 (3):311–333.
[10] Djurkovi-Djakovi O, Milenkovi V, Nikoli A, et al. Efficacy of atovaquone combined with clindamycin against murine infection with a cystogenic (Me49) strain of *Toxoplasma gondii*. J Antimicrob Chemother. 2002;50:981–987.
[11] Chirgwin K, Hafner R, Leport C, et al. Randomized phase II trial of atovaquone with pyrimethamine or sulfadiazine for treatment of toxoplasmic encephalitis in patients with acquired immunodeficiency syndrome: ACTG 237/ANRS 039 Study. Clin Infect Dis. 2002;34:1243–1250.
[12] Nagamune K, Beatty WL, Sibley LD. Artemisinin induces calcium-dependent protein secretion in the protozoan parasite *Toxoplasma gondii*. Eukaryot Cell. 2007;6:2147–2156.
[13] Innes EA. Vaccination against *Toxoplasma gondii*: an increasing priority for collaborative research? Expert Rev. Vaccines (Basel). 2010;9:1117e1119.
[14] Antczak M, Dzitko K, Długońska H. Human toxoplasmosis: searching for novel chemotherapeutics. Biomed Pharmacother. 2016;82:677–684.
[15] Abou-El-Naga IF, Mogahed NMFH. Repurposing auranofin for treatment of experimental cerebral toxoplasmosis. Acta Parasitol. 2021;1:1–10.
[16] de Clercq E. Anti-HIV drugs: 25 compounds approved within 25 years after the discovery of HIV. Int J Antimicrob Agents. 2009;33:307–320.
[17] Abou-El-Naga IF, Mady RF, Mogahed NMFH. In vitro effectivity of three approved drugs and their synergistic interaction against *Leishmania infantum*. Biomedica. 2020;1:89–101.
[18] Parikh S, Gut J, Istvan E, et al. Antimalarial activity of human immunodeficiency virus type 1. Antimicrob Agents Chemother. 2005;49:2983–2985.
[19] Sangenito LS, Menna-Barreto RFS, Oliveira AC, et al. Primary evidence of the mechanisms of action of HIV aspartyl peptidase inhibitors on *Trypanosoma cruzi* trypomastigote forms. Int J Antimicrob Agents. 2018;52:185–194.

[20] Monzote L, Rodríguez M, Alfonso Y, et al. Antiretroviral activity of protease inhibitors against *Toxoplasma gondii*. Rev Inst Med Trop. 2013;55:65–67. Sao Paulo.
[21] Abou-El-Naga IF, El Kerdany ED, Mady RF, et al. The effect of lopinavir/ritonavir and lopinavir/ritonavir loaded PLGA nanoparticles on experimental toxoplasmosis. Parasitol Int. 2017;66:735–747.
[22] Fernández-Montero JV, Barreiro P, Soriano V. HIV protease inhibitors: recent clinical trials and recommendations on use. Expert Opin Pharmacother. 2009;10:1615–1629.
[23] Shea M, Jäkle U, Liu Q, et al. A family of aspartic proteases and a novel, dynamic and cell-cycle-dependent protease localization in the secretory pathway of *Toxoplasma gondii*. Traffic. 2007;8:1018–1034.
[24] Coffey MJ, Dagley LF, Seizova S, et al. Aspartyl protease 5 matures dense granule proteins that reside at the host-parasite interface in *Toxoplasma gondii*. mBio. 2018;9:e01796–18.
[25] Hammoudi PM, Jacot D, Mueller C, et al. Fundamental roles of the Golgi-associated *Toxoplasma* aspartyl protease, ASP5, at the host-parasite interface. PLoS Pathog. 2015;11:e1005211.
[26] El-Zawawy LA, El-Said D, Mossallam SF, et al. Preventive prospective of triclosan and triclosan-liposomal nanoparticles against experimental infection with a cystogenic ME49 strain of *Toxoplasma gondii*. Acta Trop. 2015;141:103–111.
[27] Silva LA, Fernandesa MD, Machadoa AS, et al. Efficacy of sulfadiazine and pyrimethamine for treatment of experimental toxoplasmosis with strains obtained from human cases of congenital disease in Brazil. Exp Parasitol. 2019;202:7–14.
[28] Djakovic D, Milenkovic T. Murine model of drug-induced reactivation of *Toxoplasma gondii*. Acta Protozool. 2001;40:99e106.
[29] Araujo FG, Huskinson J, Remington JS, et al. Remarkable in vitro and in vivo activities of the hydroxyl-naphthoquinone 566C80 against tachyzoites and tissue cysts of *Toxoplasma gondii*. Antimicrob Agents Chemother. 1991;35:293–299.
[30] Chew WK, Wah MJ, Ambu S, et al. *Toxoplasma gondii*: determination of the onset of chronic infection in mice and the in vitro reactivation of brain cysts. Exp Parasitol. 2012;130:22–25.
[31] Araujo FG, Suzuki Y, Remington JS. Use of rifabutin in combination with atovaquone, clindamycin, pyrimethamine, or sulfadiazine for treatment of toxoplasmic encephalitis in mice. Eur J Clin Microbiol Infect Dis. 1996;15:394–397.
[32] Romand S, Pudney M, Derouin F. In vivo and in vitro activities of hydroxynaphthoquinone atovaquone alone or combined with pyrimethamine, sulfadiazine, clarithromycin, or minocycline against *Toxoplasma gondii*. Antimicrob Agents Chemother. 1993;37:2371–2378.
[33] Ferguson DJ, Hutchison WM, Pettersen E. Tissue cyst rupture in mice chronically infected with *Toxoplasma gondii*. An immunocytochemical and ultrastructural study. Parasitol Res. 1989;75:599–603.
[34] Coffey MJ, Sleebs BE, Uboldi AD, et al. An aspartyl protease defines a novel pathway for export of *Toxoplasma* proteins into the host cell. eLife. 2015;4:e10809–34.
[35] Sibley LD, Niesman IR, Parmley SF, et al. Regulated secretion of multi-lamellar vesicles leads to formation of a tubulo-vesicular network in host-cell vacuoles occupied by *Toxoplasma gondii*. J Cell Sci. 1995;108:1669–1677.
[36] Roiko MS, Carruthers VB. New roles for perforins and proteases in apicomplexan egress. Cell Microbiol. 2009;11:1444–1452.
[37] Blackman MJ. Malarial proteases and host cell egress: an 'emerging' cascade. Cell Microbiol. 2008;10:1925–1934.
[38] Hobbs CV, Tanaka TQ, Muratova O, et al. HIV treatments have malaria gametocyte killing and transmission blocking activity. J Infect Dis. 2013;208:139–148.
[39] Saag MS, Schooly RT. Antiretroviral chemotherapy. In: Remington J, Schwartz MN, editors. Current clinical topics in infectious disease. Boston: McGraw Hill Book Co; 1998. p. 154–179.
[40] Lemgruber L, Lupetti P, Martins-Duarte ES, et al. The organization of the wall filaments and characterization of the matrix structures of *Toxoplasma gondii* cyst form. Cell Microbiol. 2011;13:1920–1932.
[41] Tu V, Tomita T, Sugi T, et al. The *Toxoplasma gondii* cyst wall interactome. mBio. 2020;11:e02699–19.
[42] Fox BA, Guevara RB, Rommereim LM, et al. *Toxoplasma gondii* parasitophorous vacuole membrane associated dense granule proteins orchestrate chronic infection and GRA12 underpins resistance to host gamma interferon. mBio. 2019;10:e00589–19.
[43] Guevara RB, Fox BA, Bzik DJ. *Toxoplasma gondii* parasitophorous vacuole membrane-associated dense granule proteins regulate maturation of the cyst wall. mSphere. 2020;5:e00851–19.
[44] Fox BA, Falla A, Rommereim LM, et al. Type II *Toxoplasma gondii* KU80 knockout strains enable functional analysis of genes required for cyst development and latent infection. Eukaryotic Cell. 2011;10:1193–1206.
[45] Gold DA, Kaplan AD, Lis A, et al. The *Toxoplasma* dense granule proteins GRA17 and GRA23 mediate the movement of small molecules between the host and the parasitophorous vacuole. Cell Host Microbe. 2015;17:642–652.
[46] Paredes-Santos T, Wang Y, Waldman B, et al. The GRA17 parasitophorous vacuole membrane permeability pore contributes to bradyzoite viability. Front Cell Infect Microbiol. 2019;9:321–332.
[47] Rebello KM, Andrade-Neto VV, Zuma AA, et al. Lopinavir, an HIV-1 peptidase inhibitor, induces alteration on the lipid metabolism of *Leishmania amazonensis* promastigotes. Parasitology. 2018;145:1304–1310.
[48] Kraft TE, Armstrong C, Heitmeier MR, et al. the glucose transporter pfht1 is an antimalarial target of the HIV protease inhibitor lopinavir. Antimicrob Agents Chemother. 2015;59:6203–6209.
[49] Sa Q, Ochiai E, Tiwari A, et al. Cutting Edge: IFN-γ produced by brain-resident cells is crucial to control cerebral infection with *Toxoplasma gondii*. J Immunol. 2015;195:796–800.
[50] Divanovic S, Sawtell NM, Trompette A, et al. Opposing biological functions of tryptophan catabolizing enzymes during intracellular infection. J Infect Dis. 2012;205:152–161.
[51] Hammouda NA, Abou-El-Naga IF, Hussein ED, et al. Opsonization and intracellular killing of *Toxoplasma gondii* by human mononuclear phagocytes. J Egypt Soc Parasitol. 1995a;25:11–17.

[52] Hammouda NA, Rashwan EA, Hussien ED, et al. Measurement of respiratory burst of TNF and IL-1 cytokine activated murine peritoneal macrophages challenged with Toxoplasma gondii. J Egypt Soc Parasitol. 1995b;25:683–691.
[53] Wang X, Michie SA, Xu B, et al. Importance of IFN-gamma-mediated expression of endothelial VCAM-1 on recruitment of CD8+ T cells into the brain during chronic infection with *Toxoplasma gondii*. J Interferon Cytokine Res. 2007;27:329–338.
[54] Suzuki Y, Wang X, Jortner BS, et al. Removal of *Toxoplasma gondii* cysts from the brain by perforin-mediated activity of CD8+ T cells. Am J Pathol. 2010;176:1607–1613.
[55] Dubey JP, Lindsay DS, Speer CA. Structures of *Toxoplasma gondii* tachyzoites, bradyzoites, and sporozoites and biology and development of tissue cysts. Clinic Microbial Reviews. 1998;11:267–299.
[56] Suzuki Y, Sher A, Yap G, et al. IL-10 is required for prevention of necrosis in the small intestine and mortality in both genetically resistant BALB/c and susceptible C57BL/6 mice following peroral infection with *Toxoplasma gondii*. J Immunol. 2000;164:5375–5382.
[57] Jankovic D, Kullberg MC, Feng CG, et al. Conventional T-bet(+) Foxp3(-) Th1 cells are the major source of host-protective regulatory IL-10 during intracellular protozoan infection. J Exp Med. 2007;204:273–283.
[58] Bando H, Lee Y, Sakaguchi N, et al. *Toxoplasma* effector GRA15-dependent suppression of IFN-γ-induced antiparasitic response in human neurons. Front Cell Infect Microbiol. 2019;9:1–11.
[59] Pfefferkorn ER, Eckel M, Rebhun S. Interferon-gamma suppresses the growth of *Toxoplasma gondii* in human fibroblasts through starvation for tryptophan. Mol Biochem Parasitol. 1986a;20:215–224.
[60] Gay G, Braun L, Brenier-Pinchart MP, et al. *Toxoplasma gondii* TgIST co-opts host chromatin repressors dampening STAT1-dependent gene regulation and IFN gamma-mediated host defenses. J Exp Med. 2016;213:1779–1798.
[61] Feliu V, Vasseur V, Grover HS, et al. Location of the CD8 T cell epitope within the antigenic precursor determines immunogenicity and protection against the *Toxoplasma gondii* parasite. PLoS Pathog. 2013;9:e1003449.
[62] Salvioni A, Belloy M, Lebourg A, et al. Robust control of a brain-persisting parasite through MHC I presentation by infected neurons. Cell Rep. 2019;27:254–268.
[63] Chu HH, Chan SW, Gosling JP, et al. Continuous effector CD8(+) T cell production in a controlled persistent infection is sustained by a proliferative intermediate population. Immunity. 2016;45:159–171.
[64] Fagone P, Mangano K, Quattrocchi C, et al. Effects of NO-hybridization on the immunomodulatory properties of the HIV protease inhibitors lopinavir and ritonavir. Basic Clin Pharmacol Toxicol. 2015;117:306–315.
[65] Heimfarth L, Serafini MR, Martins-Filho PR, et al. Drug repurposing and cytokine management in response to COVID-19: a review. Int Immunopharmacol. 2020;88:e106947.
[66] Alves EAR, De Miranda MG, Borges TK, et al. Anti-HIV drugs, lopinavir/ritonavir and atazanavir, modulate innate immune response triggered by *Leishmania* in macrophages: the role of NF-κB and PPAR-γ. Int Immunopharmacol. 2015;24:314–324.